Drug Design, Development and Therapy

Dovepress
open access to scientific and medical research

Open Access Full Text Article

ORIGINAL RESEARCH

Uncovering the Potential Mechanisms of *Coptis chinensis* Franch. for Serious Mental Illness by Network Pharmacology and Pharmacology-Based Analysis

Yiyu Qi[1], Saijia Ni[2], Xia Heng[1], Shuyue Qu[1], Pingyuan Ge[1], Xin Zhao[1], Zengying Yao[2], Rui Guo[3], Nianyun Yang[1], Qichun Zhang[2], Huaxu Zhu[1]

[1]Department of Traditional Chinese Medicine Processing and Preparation, Nanjing University of Chinese Medicine, Nanjing, Jiangsu, People's Republic of China; [2]Department of Pharmacology, Nanjing University of Chinese Medicine, Nanjing, Jiangsu, People's Republic of China; [3]Department of Physiological, Nanjing University of Chinese Medicine, Nanjing, Jiangsu, People's Republic of China

Correspondence: Qichun Zhang; Huaxu Zhu, Email zhangqichun@njucm.edu.cn; zhuhx@njucm.edu.cn

Background: Serious mental illness is a disease with complex etiological factors that requires multiple interventions within a holistic disease system. With heat-clearing and detoxifying effects, *Coptis chinensis* Franch. is mainly used to treat serious mental illness.

Aim of the Study: To explore the underlying mechanisms and therapeutic effect by which *Coptis chinensis* Franch. treats serious mental illnesses at a holistic level.

Methods: A viable network pharmacology approach was adopted to obtain the potential active ingredients of *Coptis chinensis* Franch., and serious mental illnesses-related targets and signaling pathways. The interactions between crucial target HTR2A and constituents were verified by molecular docking, and the dynamic behaviors of binding were studied by molecular dynamics simulation. In addition, the anti-anxiety effect of Rhizoma Coptidis (the roots of *Coptis chinensis* Franch.) extract on lipopolysaccharide-stimulated mice was verified. The anxiety-like behavior was measured through the elevated plus-maze test, light–dark box test, and open field test. Radioimmunoassays detected the levels of interleukin-1β, tumor necrosis factor-α, interleukin-10, interleukin-4, 5-hydroxytryptamine, and dopamine in the serum, hippocampus, medial prefrontal cortex, and amygdala. Meanwhile, immunohistochemistry protocols for the assessment of neuronal loss (neuron-specific nuclear protein) and synaptic alterations (Synapsin I) were performed in the hippocampus.

Results: Based on scientific analysis of the established networks, serious mental illnesses-related targets mostly participated in the calcium signaling pathway, cyclic adenosine monophosphate signaling pathway, mitogen-activated protein kinase signaling pathway, serotonergic and dopaminergic synapse. Molecular docking and molecular dynamics simulation studies illustrated that berberine, epiberberine, palmatine, and coptisine presented favorable binding patterns with HTR2A. The in vivo experiments confirmed that Rhizoma Coptidis extract ameliorated anxiety-like behaviors by improving the survival of neurons, regulating synaptic plasticity, and inhibiting neuroinflammation.

Conclusion: These findings in the present study led to potential preventative and therapeutic strategies for serious mental illnesses with traditional Chinese medicine.

Keywords: *Coptis chinensis* Franch, serious mental illness, multitarget, network pharmacology, molecular mechanism

Background

Common serious mental illnesses (SMIs), namely, psychiatric disorders, include schizophrenia, major depressive disorder, severe anxiety, schizophreniform disorder, and psychosis;[1] these disorders dramatically reduced the patient's quality of life and caused a great burden to society.[2,3] Depression is a prevalent and debilitating SMI[3,4] with symptoms including appetite disturbance, anhedonia, sleep disturbance, hopelessness, and anergia, which severely disrupt routine

Received: 29 September 2021
Accepted: 21 January 2022
Published: 9 February 2022

Graphical Abstract

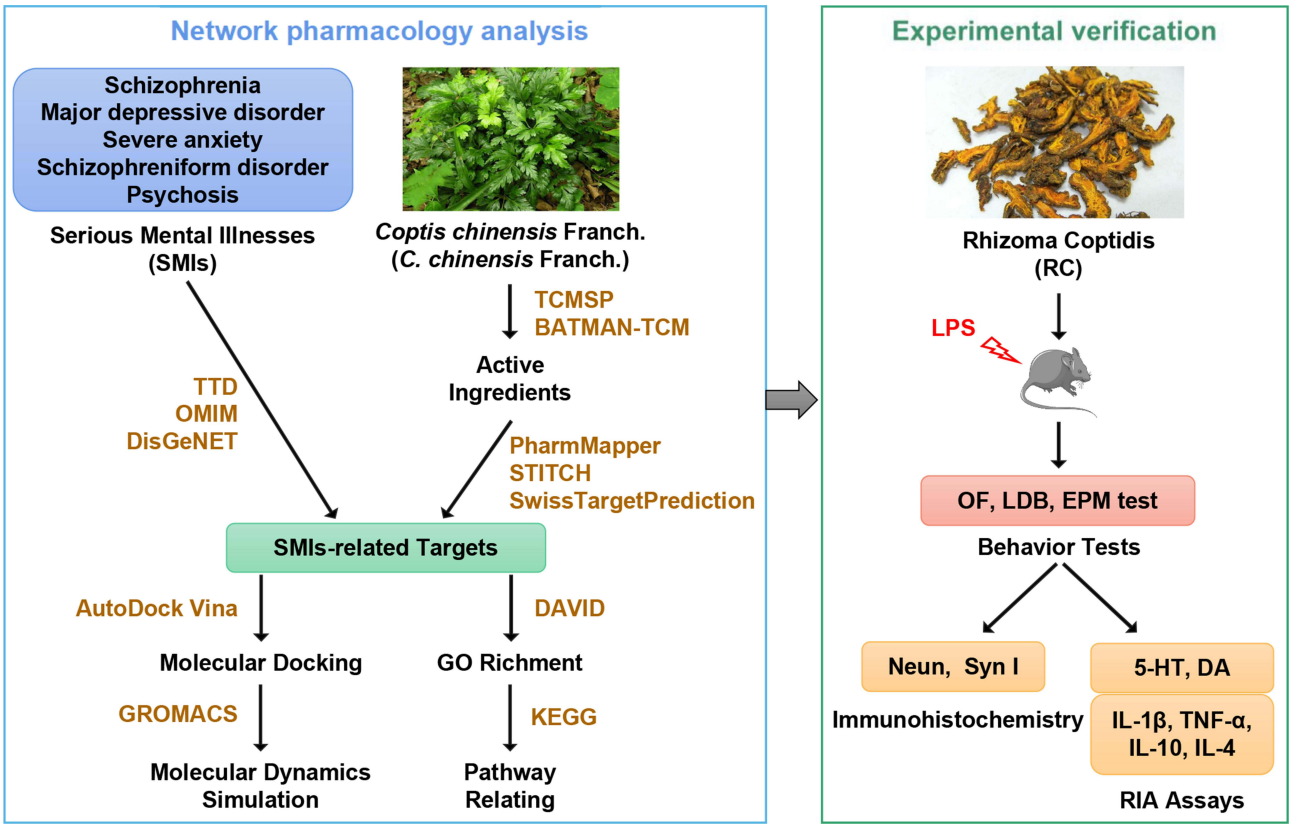

behavior and activity.[5] Schizophrenia, often consistent with depression, is fully recognized as a chronic and disabling disease,[6] with far-reaching influence on behavior, consciousness, thinking, emotions, neuro-cognition, and social functions.[7] Anxiety is the most frequent mental, emotional and behavioral problem.[2] Characterized by a persistent subjectively unpleasant state,[8–10] anxiety is highly comorbid with depression.[11,12] Moreover, anxiety is significantly related to bipolar affective disorders,[13,14] as well as physiological dysfunctions.[15] Currently, the most popular medications for SMIs are designed to regulate the function of monoamine neurotransmitters.[16,17] However, they usually act solely on a single target, and produce many side effects (for example, headache and emesis).[18–21] It is an urgent problem to find natural drugs that can exert synergistic effects.

Traditional Chinese medicine (TCM) with multi-component, multi-target and multi-pathway characteristics focuses on the overall functional state of the patients and the adjustment of their balance, which has aroused ever-increasing interest worldwide, especially for the treatment of complex diseases.[22] According to TCM theory, the pathogenesis of SMIs is always hyperactivity of heart-liver fire, restlessness of the mind, pyrogenic and burning body fluid, Qi and blood, condensing fluids to phlegm. Finally, the pathological products (fire heat and phlegm turbidity) harass the heart spirit. Hence, to ameliorate the symptoms of SMIs, soothing the liver, clearing heat, purging fire, and drying dampness to resolve phlegm are primary therapeutic strategies in TCM.

Coptis chinensis Franch. (*C. chinensis* Franch.) is a representative herb with the function of clearing heat and removing toxicity. Active ingredients of *C. chinensis* Franch. and several traditional formulae containing *C. chinensis* Franch. exhibit positive therapeutic effects on SMIs.[23–28] Therefore, a comprehensive detection method based on network pharmacology and experimental evidence was established in this study to form a more complete picture of the physiological pathways through which *C. chinensis* Franch. may act to treat SMIs, thereby improving the chances of

producing effective targeted therapies. Active components, candidate targets, and biological pathways were successfully identified. Then, the molecular mechanism underlying the effects of compounds in *C. chinensis* Franch. on key target was further validated by performing molecular docking and molecular dynamics (MD) simulation. The results of in vivo experiments indicated that Rhizoma Coptidis (RC) extract ameliorates anxiety-like behaviors in lipopolysaccharide (LPS)-induced mice by regulating neurochemistry, improving inflammation, and modulating synaptic plasticity. This study preliminarily explored the mechanism of *C. chinensis* Franch. in the treatment of SMIs, and provided a research basis for the development of anti-SMIs drugs.

Materials and Methods

Network Pharmacology Assay

Software and Database

The databases for the assay of network pharmacology were listed below: traditional Chinese medicine systems pharmacology (TCMSP) database (http://lsp.nwu.edu.cn/tcmsp.php), BATMAN-TCM database (http://bionet.ncpsb.org/batman-tcm/), PharmMapper server (http://lilab.ecust.edu.cn/pharmmapper/index.php), PubChem database (https://pubchem.ncbi.nlm.nih.gov/), Search Tool for Interacting Chemicals (STITCH) server (http://stitch.embl.de/), SwissTargetPrediction server (http://www.swisstargetprediction.ch/), Online Mendelian Inheritance in Man (OMIM) database (http://www.omim.org/), Therapeutic Target Database (TTD) (http://bidd.nus.edu.sg/BIDD-Databases/TTD/TTD.asp), DisGeNET database (http://www.disgenet.org), KEGG database (https://www.kegg.jp/), Database for Annotation, Visualization and Integrated Discovery (DAVID) webservers (https://david.ncifcrf.gov/), and Cytoscape 3.2.1 software.

Active Ingredients Sifting

First, the Chinese name of *C. chinensis* Franch. was submitted to the TCMSP,[29] and active components with oral bioavailability (OB)≥30% and drug-likeness (DL)≥0.18 were chosen.[30,31] In addition, the Pinyin of *C. chinensis* Franch. was sent to the BATMAN-TCM,[32] and active ingredients with score ≥ 20 and $p \leq 0.05$ were selected. Combined with the above results, the active components of *C. chinensis* Franch. were obtained.

Ingredient-Related and Disease-Associated Target Prediction

The active ingredients were submitted to the PubChem database to obtain the 3D structures and canonical SMILES. All 3D structures were sent to the PharmMapper server.[33] The top 50 targets served as potential targets for each active ingredient based on the fit score. Meanwhile, all canonical SMILES were submitted to various servers viz. Swiss Target Prediction[34] and STITCH server.[35] Targets that appeared in the above three databases were selected. For the acquisition of SMIs-related targets, TTD,[36] DisGeNET database,[37] and OMIM database[38] were employed.

Enrichment Analysis and Network Construction

The DAVID[39] was used to achieve Gene Ontology (GO) enrichment analysis. The biological process (BP), molecular function (MF), and cellular component (CC) results were appeared by GraphPad Prism 8.3.0 software. The Kyoto Encyclopedia of Genes and Genomes (KEGG) pathway enrichment analysis was also extracted from DAVID. The compound-target (C-T) and target-pathway (T-P) visualized networks were constructed through Cytoscape 3.2.1 software.[40]

Contribution Indexes Calculation

To evaluate the contribution of every effective compound of *C. chinensis* Franch. in treating SMI effectively, a contribution index (CI) on the basis of network-based efficacy (NE) weighted by the literature was devised and calculated by the following two equations:[41]

$$\mathbf{NE(j)} = \sum_{\mathbf{i}=1}^{\mathbf{n}} \mathbf{d_i} \tag{1}$$

$$\mathbf{CI(j)} = \frac{\mathbf{c_j} \times \mathbf{NE(j)}}{\sum_{\mathbf{i}=1}^{\mathbf{m}} \mathbf{c_i} \times \mathbf{NE(i)}} \times 100\% \tag{2}$$

In these equations, **n** represents the number of targets associated with the component **j** in the C-T network; $\mathbf{d_i}$ represents the degree of the target **i** associated with the component **j** in the T-P network; $\mathbf{c_i}$ represents the number of SMI-related studies of component **i**; and **m** represents the number of active compounds. Several keywords were used for the SMI-related literature-mining approach: psychosis, psychotic, mental disease, mental disorder, mental illness, schizophrenia, depressive, antidepressant, depressed, depression, and anxiety. The number of papers with corresponding keywords in the title/abstract published between 1991 and 2021 was acquired from the PubMed database. When the sum of CIs of the top N compounds was greater than 85%, these compounds were deemed to contribute the most to the treatment of SMIs.[41]

Molecular Docking and MD Simulation

Molecular docking was used to predict interactions between the key target and *C. chinensis* Franch. active compounds. The initial structure of HTR2A (PDB ID: 6A94) was downloaded from the RCSB Protein Data Bank (http://www.rcsb.org). Substrates were docked into the active site of protein using AutoDock Vina tool[42] in Chimera.[43] Next, to understand the dynamic behavior of ligand at the active site of the protein and further confirm the stability of complex, the docking poses with the highest docking scores were used for the subsequent MD simulations. The general AMBER force field[44] was used for substrates, while the partial atomic charges were obtained from the RESP method by Multwfn.[45] The systems were solvated in a rectangular box of TIP3P [46] waters extending up to a minimum cutoff of 10 Å from the protein boundary. The AMBER ff14SB force field[47] was employed for the protein in all of the MD simulations. The initial structures were fully minimized using combined steepest descent and conjugate gradient method. The systems were then gently annealed from 10 to 300 K under canonical ensemble for 0.5 ns with a weak restraint of 15 kcal/mol/Å. 500 ps of density equilibration was performed under isothermal-isobaric ensemble at target temperature of 300 K and a target pressure of 1.0 atm using Langevin thermosta[48] and Berendsen barostat[49] with a collision frequency of 0.002 ns and a pressure-relaxation time of 0.001 ns. After proper minimizations and equilibrations, a productive MD run of 100 ns was performed for all the complex systems. Finally, the MD simulations were performed with GROMACS (version 2020.3)[50] MM/PB(GB)SA calculations within the gmx_mmpbsa community.[51]

Animal Experiments

Chemicals and Material

RC (batch number, 1711028050) was purchased from Anhui Huizhongzhou TCM Pieces Co., Ltd. (Anhui, China) and authenticated by Prof. Qi-nan Wu (College of Pharmacy, Nanjing University of Chinese Medicine, Nanjing, China). Voucher specimens were deposited at the Museum of Materia Medica, Nanjing University of Chinese Medicine. Diazepam (DZP) was purchased from Huazhong Pharmaceutical Co., Ltd. (Hubei, China). LPS (from Escherichia coli, serotype 0111: B4) and pentobarbital sodium were from Sigma-Aldrich (St. Louis, MO, USA). Radioimmunoassay (RIA) kits for 5-HT (20210202), DA (20210129), IL-1β (20210201), TNF-α (20200130), IL-10 (20200201), and IL-4 (20200203) were purchased from Beijing Sino-UK Institute of Biological Technology (Beijing, China). Two primary antibodies were used in the study: rabbit anti-NeuN (Abcam, ab236870, 1:40000) and rabbit anti-Syn I (Abcam, ab254349, 1:10000).

Preparation of the RC Extract

The extraction of RC solution was based on the preparation of the standard decoction of RC pieces mentioned by Guo et al.[52] Briefly, 50 g RC was soaked in 7 times of water for 30 min and then boiled for 30 min. Then, dregs were boiled again in 6 times of water for 20 min. We combined the two filtrates and concentrated by a rotary evaporator and frozen at -80°C for at least 12 h. After lyophilization, 8.98 g of lyophilized powder was obtained.

Animals and Treatments

SPF male C57BL/6 mice (12–14 weeks, 18–22 g), were purchased from Animal Multiplication Center of Qinglong Mountain, Nanjing, China) and housed in a temperature and relative humidity-controlled room (21±2°C, 60±10%) with a 12-h light/dark cycle (lights on at 07:00 a.m.). Mice were randomly divided into 6 groups with 10 mice each after one week of acclimation. Drug treatment groups were orally administered DZP (2 mg/kg/day, dissolved in 0.5% CMC-Na) and RC (146, 292 and 584 mg/kg/day, dissolved in 0.5% CMC-Na) for 6 days. On the 5th day, 1 h after administration,

all mice except the control group were intraperitoneally exposed to LPS (0.83 mg/kg, i.p., dissolved in sterile saline), which induces anxiety.[53] All drugs were administered at 0.1 mL/10 g body weight. The RC dose was calculated according to the dosage stipulated in the Chinese Pharmacopoeia 2020[54] and the dosage conversion relationship between mice and humans. Animal welfare and experimental procedures were strictly performed in accordance with the Guide for the Care and Use of Laboratory Animals (US National Research Council, 1996). The Animal Care and Use Committee of Nanjing University of Chinese Medicine approved the protocol and the total number of mice used in this study.

Behavioral Tests

Behavioral tests were performed in a dimly lit, quiet, and isolated room by an experimenter blinded to the identity of the mice. For each behavioral test, mice were placed in the test preparation chamber 1 h in advance. Behavioral apparatuses were cleaned with 75% v/v ethanol solution and dried with absorbent cotton after each trial. The open field (OF) test, light–dark box (LDB) test, and elevated plus maze (EPM) test were measured at 4, 7, and 24 hours after drug administration in saline or LPS, respectively. This time-window was carefully chosen to enable behaviors to be assessed at the peak of LPS-induced sickness and proinflammatory cytokine release.[55]

OF Test

OF test is widely carried out as a screening experiment for anxiety-related behavior.[56] The OF device (40 × 40 × 30 cm) was evenly divided into 16 squares (10 × 10 cm). The four squares in the center were considered the central area, while the remaining 12 squares were considered the periphery.[57] A video camera was placed above the center. Each mouse was placed in the central area and allowed to explore for 5 min. The total distance traveled in the OF, frequency of entry into the central area, distance traveled and time spent in the central area were recorded using the Video Analysis System for Animal Behavior (JL, Shanghai, PRC). Subsequently, the percentage of distance, and the time spent in the central area were statistically analyzed.

LDB Test

The LDB test was carried out following previous protocols.[58,59] The testing apparatus consists of two different boxes: a light box (27 × 27 × 27 cm; white walls and bright) and a dark box (27 × 18 × 27 cm; black walls and dark). Between the two compartments, there was an opening (6 × 6 cm). A video camera was located above the apparatus. Each mouse was placed in the light box facing the opening and allowed to explore the arena for 5 min. The number of light–dark box transitions and the time spent in the light box were recorded. Subsequently, the percentage of time spent in the light box was statistically analyzed.

EPM Test

The EPM, one of the most popular behavioral assays, is ground on rodents' innate fear of open, elevated areas.[60] When faced with a choice, mice showed a preference for staying in the safe environment (closed arms) over the dangerous one (open arms).[61] Following a previously published protocol,[62] the EPM consists of four arms extending from a central platform (5 × 5 cm), including two open arms (30 × 5 cm) and two closed arms (30 × 5 × 15.25 cm high walls), and the whole apparatus was elevated 40 cm above the floor. A video device was placed above the central platform. Each mouse was placed in the central region, facing an open arm, and allowed to explore freely for 5 min. The numbers of entries into and the time spent in open and closed arms were counted[63] by the Video Analysis System for Animal Behavior (JL, Shanghai, PRC). Subsequently, the percentage of entry into open arms and the percentage of time spent in open arms were calculated. Mice that fell out of the EPM were not statistically analyzed.

RIA

After behavioral experiments, mice from the control, model, and RC (292 mg/kg) groups (n = 6) were anesthetized with pentobarbital sodium (50 mg/kg, 0.05 mL/10 g, i.p.). Blood samples were centrifuged (3500 rpm, 10 min, 4°C) to obtain the serum. Then, the animals were euthanized by cervical dislocation, and their brain was taken out, the hippocampus, mPFC, and amygdala were immediately separated on ice. Proinflammatory cytokine (IL-1β and TNF-α), anti-

inflammatory cytokine (IL-10 and IL-4), and neurotransmitter (5-HT and DA) RIA assays were performed according to the manufacturers' instructions. All analyses were performed twice.

Immunohistochemistry

Four mice from the control, model, and RC (292 mg/kg) groups were anesthetized with pentobarbital sodium (50 mg/kg, 0.05 mL/10 g, i.p.) and underwent transcardiac perfusion with 50 mL saline and then 50 mL 4% paraformaldehyde. The brain samples were taken out rapidly and embedded in paraffin blocks using a paraffin embedding station (Leica Biosystems Nussloch GmbH, Leica EG1150H, Germany), followed by sectioned (5 μm) using a rotary microtome (Leica Biosystems Nussloch GmbH, Leica RM2245, Germany). First, the slices were placed in an oven at 60°C for 20–30 min. After dewaxing and hydration with two times xylene (10 min), two times absolute ethanol (5 min), 95% ethanol (10 min), 80% ethanol (10 min), and two times distilled water (1 min), the slices were treated with 3% H_2O_2 solution (10 min). Then, antigen retrieval was obtained from a water bath (≥95°C, 30 min) in citrate buffer (0.01 M, pH 6.0) followed by blocking in 5% BSA (20 min). Primary antibodies, including NeuN and Syn I, were used to incubate the sections at 4°C overnight. Sections were incubated with secondary antibodies for 4 h at room temperature. Afterward, the tissue was incubated with substrate chromogenic solution (10 min) (BOSTER, AR1022) and stained with hematoxylin (5 min). After being differentiated with 1% hydrochloric acid alcohol (20 s), the sections were successively subjected to 80% ethanol (10 s), 95% ethanol (10 s), two times anhydrous ethanol (10 min), and two times xylene (10 min) and then sealed with neutral gum. Image-Pro® Plus (6.0.0.260) was employed to calculate the mean integral optical density (IOD) of CA1, CA3, and dentate gyrus (DG) of each slice.

Statistical Analysis

All data were statistically analyzed using SPSS 17.0 software. Data distribution was assessed using the Shapiro–Wilk test and Q-Q plots (Supplementary Figure 1). Comparisons between groups were performed with one-way ANOVA with Tukey's or Dunnett's post hoc multiple comparison tests. Data are expressed as the mean±SD. Differences were considered to be significant when $p<0.05$ or $p<0.01$.

Results

Network Pharmacology Assay

Active Ingredients and Targets of *C. chinensis* Franch. On SMIs

When a single herb contains a considerable number of compounds, virtual screening approaches are helpful to distinguish active ingredients. Consequently, 14 ingredients with potent pharmacological activities were selected (Supplementary Table 1), such as berberine (MOL01, OB%=36.86%, and DL = 0.78), epiberberine (MOL04, OB%=43.09%, and DL = 0.78), palmatine (MOL10, OB% = 64.60%, and DL = 0.65), and coptisine (MOL12, OB%=30.67%, and DL = 0.86). Meanwhile, these alkaloids account for large amounts in *C. chinensis* Franch.

In order to obtain the matching targets of the active compounds of *C. chinensis* Franch. for its therapeutic benefit, a robust in silico approach combined with the chemometric method and information integration was implemented. Several predictive models, including STITCH, Swiss Target Prediction, and the PharmMapper server, were employed to predict 216 targets that interacted with the aforementioned 14 active ingredients. In addition, the TTD, DisGeNET, and OMIM databases were also employed to predict 988 targets related to SMIs. Finally, 43 targets were kept as the key targets for *C. chinensis* Franch. and SMIs (Supplementary Table 2).

Compound-Target Network and GO Enrichment Analysis of Predicted Targets of *C. chinensis* Franch

A bipartite graph of the C-T network was constructed to visualize and analyze the relationships between active ingredients and the corresponding targets (Figure 1A). This Figure consisted of 64 nodes connected by 251 edges. Compounds with high interconnection degrees, such as (R)-canadine (degree = 25), palmatine (degree = 20), berberine (degree = 20), coptisine (degree = 19), epiberberine (degree = 19), and berberrubine (degree = 19), were responsible for the high interconnection of the C-T network.

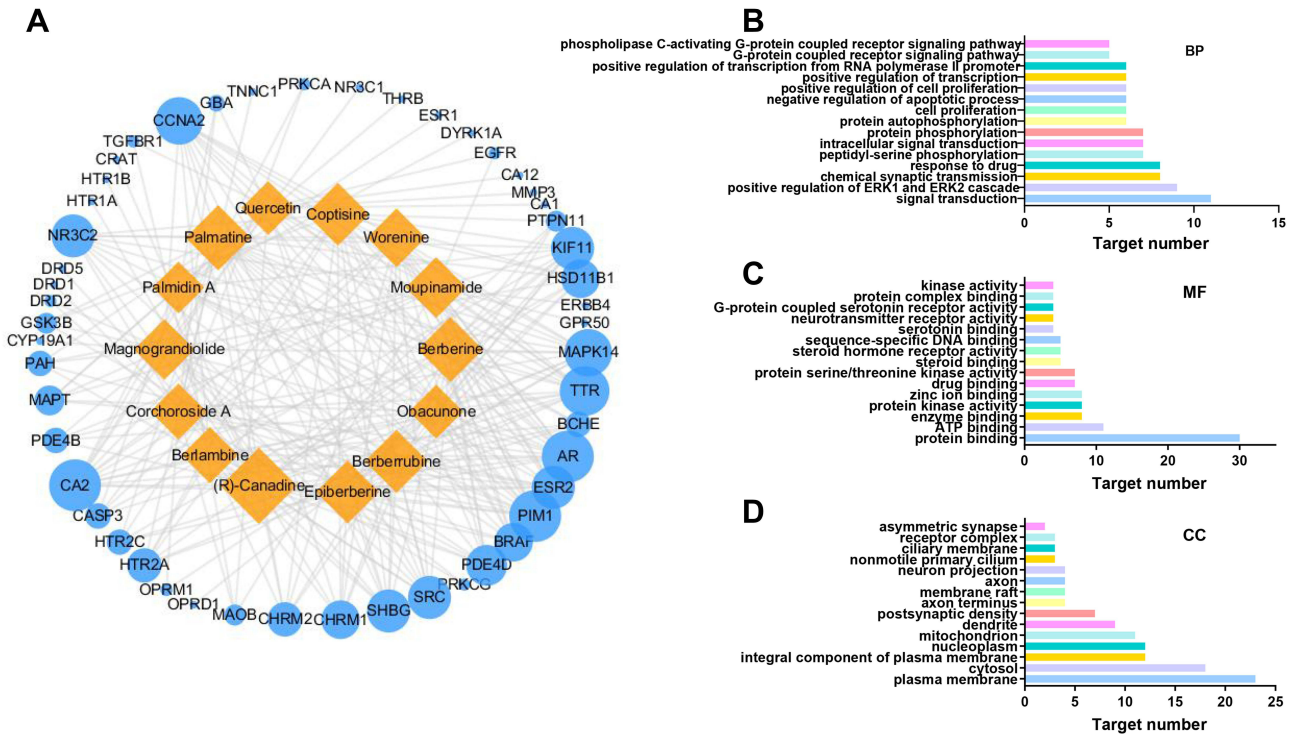

Figure 1 (**A**) C-T network of *C. chinensis* Franch. on SMIs. The yellow rectangle and blue circle represent the components and targets, respectively, and the size of notes represents the degree value; (**B**) BP, (**C**) MF, and (**D**) CC in GO enrichment analysis.

The 43 targets associated with *C. chinensis* Franch. and SMIs were submitted to DAVID bioinformatics resources for GO enrichment. The BP, MF, and CC enrichment results were visualized with GraphPad Prism 8.3.0 software. The terms of the top 15 significantly enriched in BP, MF, and CC with $p<0.05$ were listed (Figure 1B–D). Strikingly, the selected targets were associated with signal transduction, positive regulation of the ERK1 and ERK2 cascades, chemical synaptic transmission, intracellular signal transduction, and cell proliferation in BP, which were closely associated with the pathogenesis of SMIs.

KEGG Enrichment and Target-Pathway Network Analysis of Predicted Targets of *C. chinensis* Franch

A total of 32 KEGG pathways with $p<0.05$ were obtained (Supplementary Table 3). Afterward, a bipartite T-P network was built (Figure 2A). The pathways are mainly involved in signaling transduction (eg, cAMP signaling pathway, MAPK signaling pathway, and calcium signaling pathway), neurological system (eg, neuroactive ligand–receptor interaction, serotonergic synapse, and dopaminergic synapse), and endocrine system (eg, thyroid hormone signaling pathway). Among these KEGG pathways (Supplementary Table 3), those closely related to SMIs were selected as the significant pathways for further analysis. As shown in the compressed pathway (Figure 2B), C. *chinensis* Franch. modulates neurotransmitters and/or their receptors and the pivotal nodes of the following pathways, which contribute to regulating the process of neuron proliferation/differentiation, neuroinflammation, cell survival/metabolism, synaptic plasticity, and axonal outgrowth.

CI Analysis to Decipher the Role of Active Ingredients of *C. chinensis* Franch

The CI of each active ingredient was proposed based on network efficacy weighted by the literature. The calculated results (Figure 3) showed that ten compounds, magnograndiolide (MOL08, CI = 11.48%), (R)-canadine (MOL05, CI = 10.01%), coptisine (MOL12, CI = 8.92%), palmatine (MOL10, CI = 8.43%), berberine (MOL01, CI = 8.12%), epiberberine (MOL04, CI = 7.81%), and berberrubine (MOL03, CI = 7.08%), primarily contributed to the therapeutic

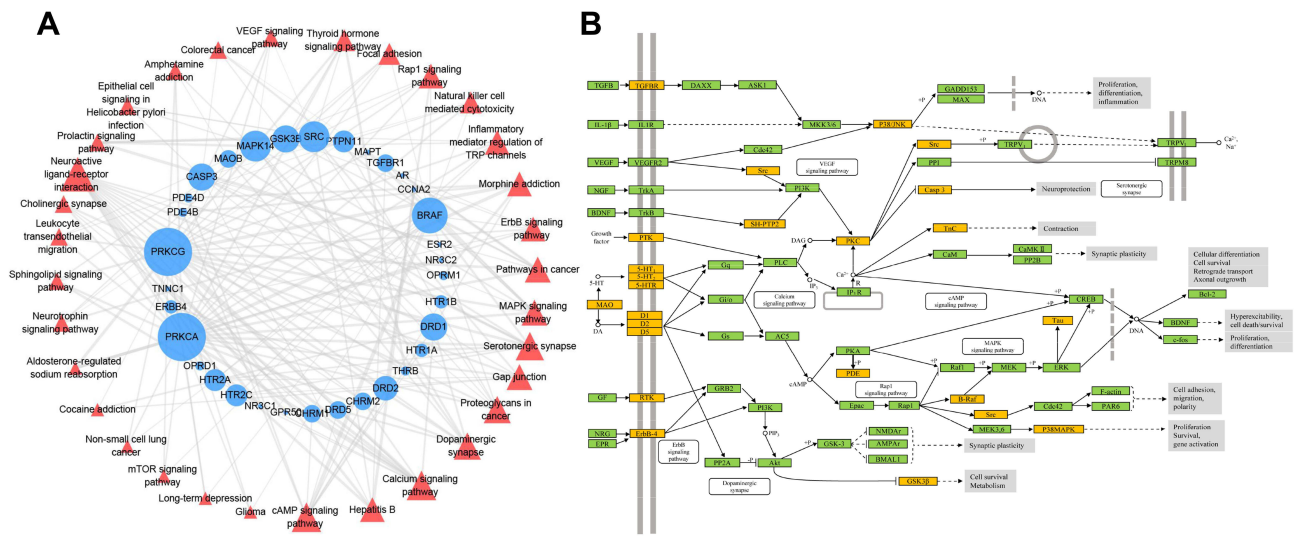

Figure 2 (**A**) T-P network of *C. chinensis* Franch. on SMIs. The blue circle and red triangle represent the targets and pathways, respectively, and the size of notes represents the degree value; (**B**) Distribution of partial targets (marked in yellow) of *C. chinensis* Franch. on the merged pathway.

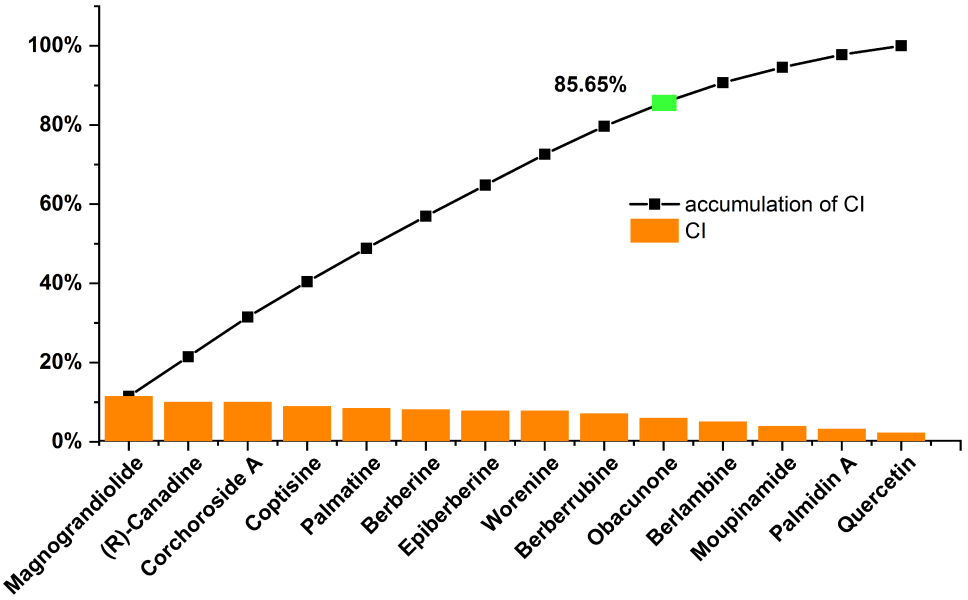

Figure 3 The CI and accumulative CI of active ingredients in *C. chinensis* Franch. The accumulative CI greater than 85% is marked bright green.

effects of *C. chinensis* Franch. reaching the sum of CIs of 85.65%. Therefore, in view of the results mentioned above, these active ingredients were considered impactful in *C. chinensis* Franch. in the treatment of SMIs.

Molecular Docking and MD Simulation of *C. chinensis* Franch. Active Compounds Binding to Hub Target

The current study predicts that HTR2A is a common target for the four active components of *C. chinensis* Franch. (berberine, epiberberine, palmatine and coptisine), and the serotonergic synapse that HTR2A participates in is an important pathway involved in SMIs. Therefore, molecular docking was performed between these four active ingredients and HTR2A. Analysis of the binding pattern of each complex revealed that each ligand was embedded in the active pocket of HTR2A and interacted with multiple residues through van der Waals, carbon-hydrogen bond, pi-sigma, pi-alkyl, etc. These interactions make the structure tend to be stable (Figure 4A–D).

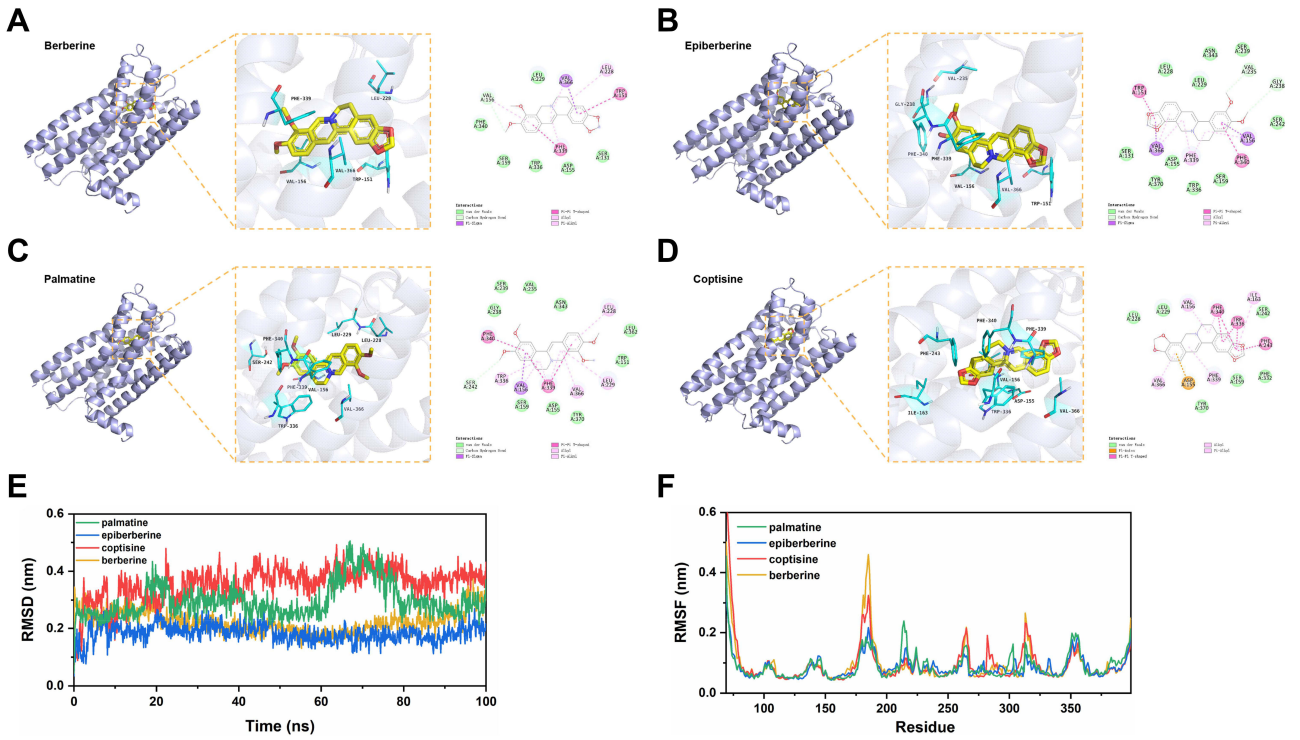

Figure 4 Predicted binding mode and MD simulation study of activity ingredients with HTR2A. The overall structure, 3D partial view and 2D binding mode of (**A**) berberine-HTR2A, (**B**) epiberberine-HTR2A, (**C**) palmatine-HTR2A, and (**D**) coptisine-HTR2A complex; (**E**) Stability assessment of four complexes by RMSD; (**F**) RMSF for each residue in four complexes.

Then, MD simulation studies were employed to investigate the molecular stability of the complexes and dynamic trajectories of interactions. Root mean square deviation (RMSD) is a commonly used quantitative measure of the similarity between two superimposed atomic coordinates.[64] The RMSD value of the berberine-HTR2A complex showed a general trend of slowly decreasing before 60 nm and then slowly increasing after 60 nm, without a large fluctuation. In the whole simulation process, the RMSD profile of the epiberberine-HTR2A complex is mainly stable at 0.2 nm. The RMSD value of palmatine-HTR2A fluctuated around 0.3 nm in general, but the structure moderately increased to 0.5 nm at 70 ns and stabilized between 0.2 and 0.3 nm after 80 ns. The coptisine-HTR2A complex, however, had a relatively high RMSD value compared to the other complexes and showed a slow increase up to 80 ns, after which it stabilized between 0.3 and 0.4 nm (Figure 4E). These results indicated that the four complexes promote conformational stability and are probably due to favorable interactions at the binding site of HTR2A.

For flexible molecules, the function of proteins depends largely on the conformation changes of different molecules.[65] To better understand the structural changes and conformational flexibility of proteins in complexes, root mean square fluctuation (RMSF) was performed to explore fluctuations of each residue in the simulation procedure. The RMSF profiles of the four protein-ligand complexes were similar, mostly within the range of 0.05 to 0.2 nm. Compared to other compounds, the epiberberine-binding site of HTR2A exhibits fewer conformation fluctuations (Figure 4F).

Finally, MM-PB(GB)SA method was used to calculate the binding free energy, and the key amino acid residues in the protein–ligand interaction were determined according to the contribution of amino acid residues to the binding free energy. The binding free energy of berberine, epiberberine, palmatine, and coptisine with HTR2A were -39.5, -32.7, -42.5, and -29.7 kcal/mol, respectively. Amino acid residues, including Val156, Leu228, Phe339, and Val366 contributed significantly (Supplemental Figure 2). These amino acid residues are hydrophobic and form pi-alkyl interactions with four compounds (Figure 4A–D).

Animal Experiments

Effect of RC Extract on the Behaviors of LPS-Induced Anxiety Mice

As mentioned in the previous article, anxiety is a more common disease and highly related to other SMIs. Subsequently, anti-anxiety studies of water extract of RC (the roots of *C. chinensis* Franch.) were carried out. Acute treatment with LPS is frequently used in animal models to investigate the biochemical mechanisms of anxiety-like behaviors.[66–70] Details on the experimental processing and behavior analysis are shown in Figure 5A. The OF test was performed to detect the locomotor activity of mice. RC extract treatment significantly increased the total distance traveled during the 5-minute session (Figure 5B and C). Movement trending towards the center area was observed. In comparison to the control, the total distance traveled in the OF, the number of entering central field, the percentage of traveling distance traveled, and the percentage of time spent in the central field in the model group were reduced by 73.22%, 90.63%, 83.30%, and 93.07%, respectively, while those in the RC extract intervention group were significantly improved (Figure 5D–F).

LPS-treated mice had significantly different behaviors in the LDB test compared with the mice in the control and DZP or RC extract group. The number of light–dark transitions was increased by at least 2.7 times in the RC extract-treated groups in comparison to the LPS-treated group (Figure 6A). The residence time in the light box of the RC group was at least 35.74% higher than that of mice in the LPS-treated group (Figure 6B).

In the EPM test, RC extract treatment significantly improved the activity of mice in the open arms (Figure 6C). The results demonstrated that the percentage of entering the open arms and the time spent in the open arms of the model mice were reduced by 65.39% and 72.66% in comparison to the control, respectively. Mice treated with RC extract, especially 292 mg/kg RC extract, significantly enhanced the percentage of entering and the time spent in open arms (Figure 6D and E).

Effects of RC Extract on Neurotransmitter and Cytokine Levels in LPS-Induced Anxiety Mice

Results of neurotransmitter concentration assay showed that the 5-HT and DA concentrations were significantly aggrandized in the serum, hippocampus, mPFC, and amygdala after LPS administration (Figure 7A and B). After the administration of LPS, the concentrations of IL-1β and TNF-α were significantly higher than mice in the normal controls (Figure 7C and D). Analysis of IL-10 and IL-4 levels revealed a significant reduction in the LPS-treated group compared with the control mice (Figure 7E and F). However, RC extract (292 mg/kg) treatment resulted in a decrease in 5-HT and DA in these three regions and serum (Figure 7A and B). In addition, the levels of pro-inflammatory factors and anti-inflammatory factors were restored in animals treated with RC extract (292 mg/kg) (Figure 7C–F).

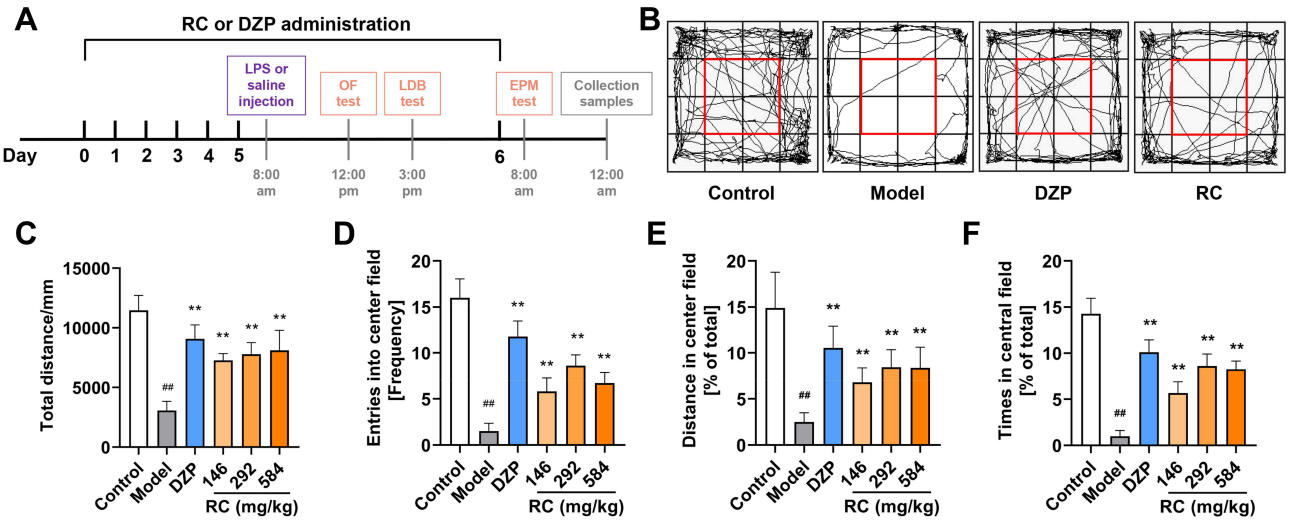

Figure 5 OF test results showing the effect of RC extract on the behaviors of LPS-induced anxiety mice. (**A**) Schematic diagram of the experimental process; (**B**) Representative movement traces (black lines) for control, model, DZP, and RC group mice in OF. Red rectangle marks the central field (25% of total area); (**C**) Total distance covered by mice; (**D**) Frequency of entering the central field; (**E**) Distance traveled in the central field; (**F**) Percentage of time mice spent in the central field. Data are from n=10 mice per group. Mean±SD plotted (Control vs Model, $^{\#\#}p<0.01$; Model vs DZP or RC, $^{**}p<0.01$).

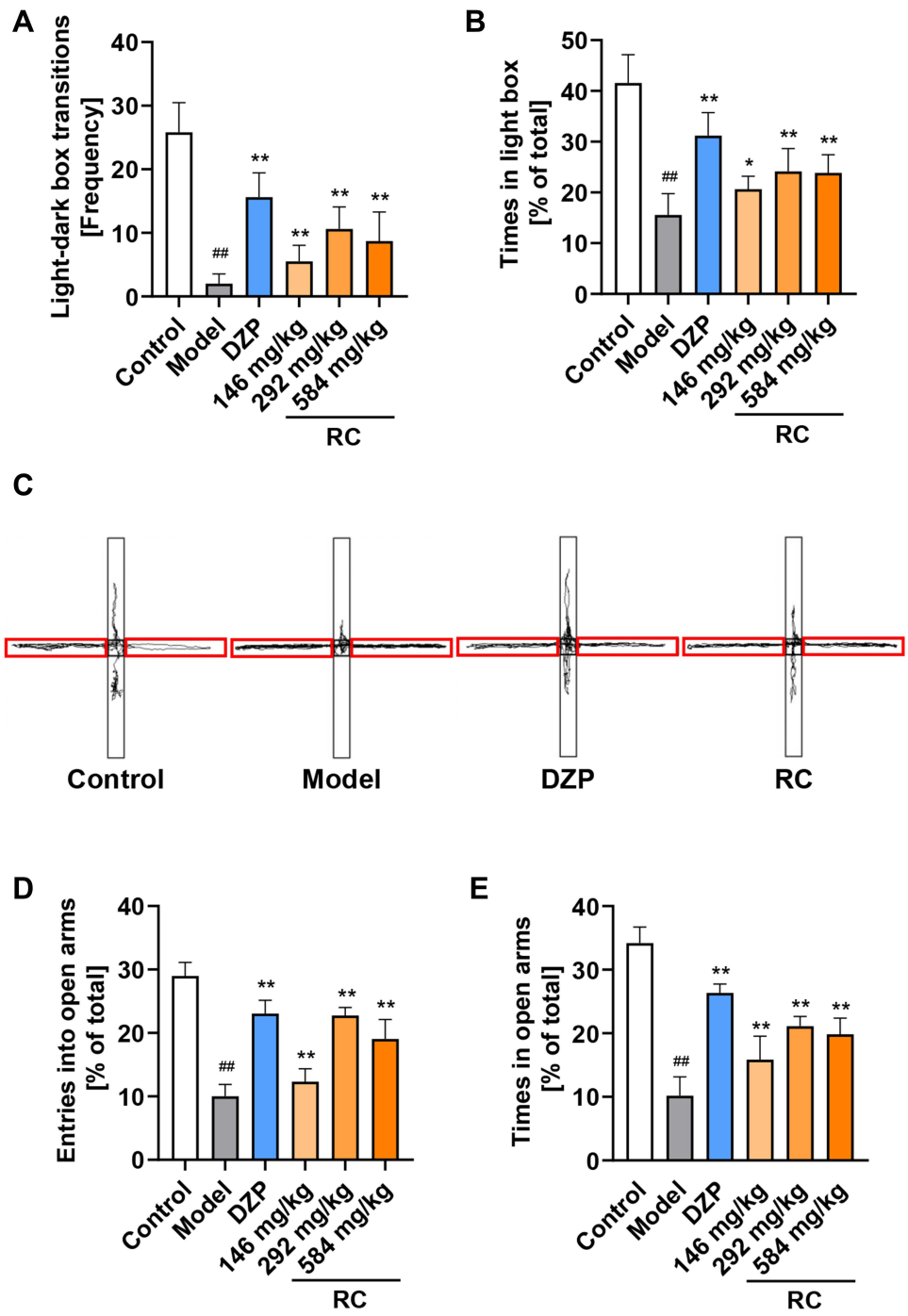

Figure 6 LDB and EPM test results show the effect of RC extract on the behaviors of LPS-induced anxiety mice. (**A**) Frequency of light and dark chamber shuttling; (**B**) Percentage of time mice spent in the light chamber; (**C**) Representative movement traces (black lines) for control, model, DZP, and RC group mice in EPM. Closed arms of the maze are indicated by red brackets; (**D**) Percentage of times the mice entered the open arms; (**E**) Percentage of time mice spent in open arms. Data are from n=10 mice per group. Mean±SD plotted (Control vs Model, $^{\#\#}p<0.01$; Model vs DZP or RC, $^{*}p<0.05$, $^{**}p<0.01$).

Effect of RC Extract on Neuronal Loss and Synaptic Alterations in LPS-Induced Anxiety Mice

NeuN, the marker of mature neurons, modulates synaptic plasticity; neurons play important roles in anxiety.[71] In the model group, NeuN-positive neurons in three regions were reduced, whereas, after RC extract (292 mg/kg) treatment, NeuN-positive cells increased in these three regions (Figure 8A).

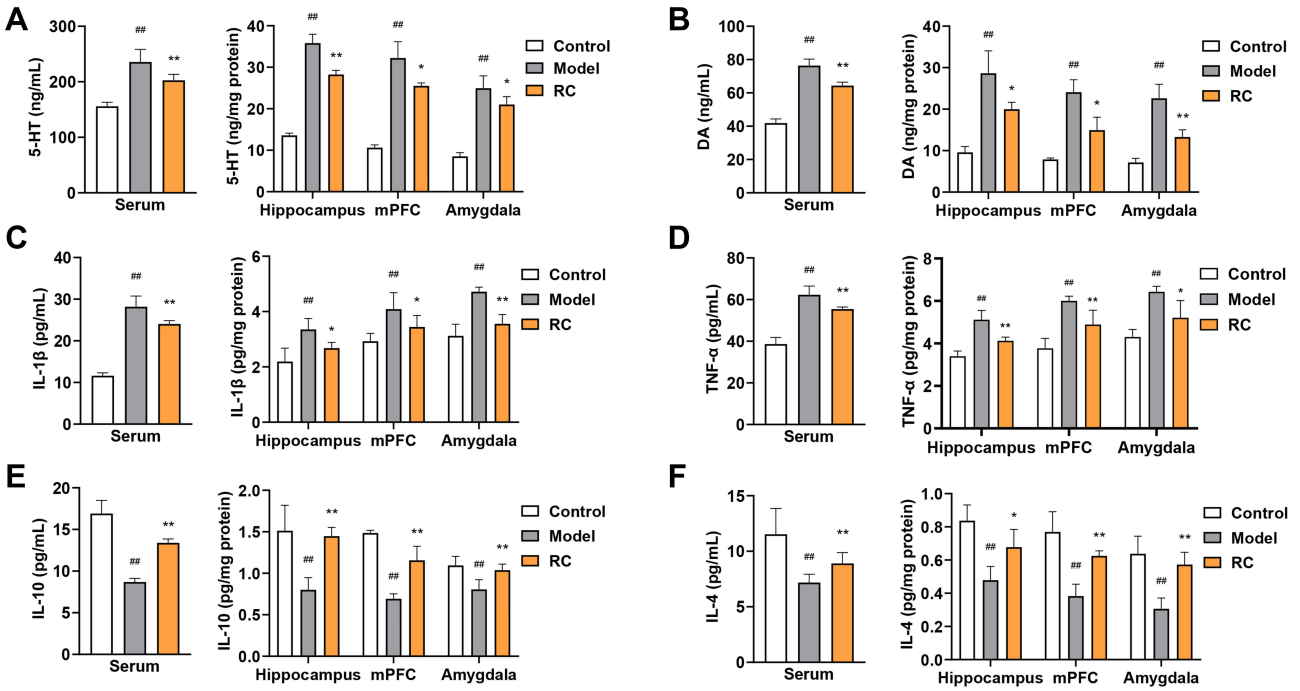

Figure 7 Effect of RC extract on neurotransmitter and cytokine levels in LPS-induced anxiety mice. Levels of (**A**) 5-HT, (**B**) DA, (**C**) IL-1β, (**D**) TNF-α, (**E**) IL-10, and (**F**) IL-4 in the serum, hippocampus, mPFC, and amygdala of control, model, and RC group mice. Data are from n=6 mice per group. Mean±SD plotted (Control vs Model, $^{\#\#}p<0.01$; Model vs RC, $^{*}p<0.05$, $^{**}p<0.01$).

Emotion is modulated by synaptic plasticity, reflecting synaptic function. NeuN has a significant influence on neurodevelopment and synaptic plasticity in the hippocampus, which is implicated in the regulation of emotion.[72] To further determine whether the synaptic function was affected by decreased NeuN expression in LPS-induced anxiety mice, the level of SynI, a phosphate protein that can regulate the release of neurotransmitters, was measured. It was found that the level of SynI was significantly reduced in the CA1, CA3, and DG of model group mice (Figure 8B). RC extract (292 mg/kg) administration increased SynI levels in these three regions of the hippocampus (Figure 8B).

Discussion

Since *C. chinensis* Franch. clears away the heart fire, eliminates the dampness, nourishes the heart to tranquilize, quenches the fire, and counteracts the poison, it has long been used to treat palpitations, vexation, insomnia, and loss of consciousness.[73] Clinically, TCM formulas with *C. chinensis* Franch. as the main medicine, such as Huanglian-Wendan decoction[74] and Huanglian-Ejiao decoction,[75] were effective in treating anxiety. Huanglian-Ejiao decoction can also improve the depression of patients.[76] Currently, berberine has proven to be a useful drug for treating or alleviating mental illness, given that it has similar anti-anxiety effects on anxiety-related behavioral and biochemical indicators.[77] Besides, berberine can improve the motor impairment and cognitive impairment caused by MK-801, indicating that timely administration of berberine may be a potential method for the settlement of schizophrenia.[78] Thus, the present study preliminarily explored the mechanism of *C. chinensis* Franch. in the treatment of SMIs.

DA receptors of dopaminergic synapses and 5-HT receptors of serotonergic synapses are predicted targets and biological pathways for the efficacy of *C. chinensis* Franch. Recent network pharmacology studies on TCM treatment of SMIs[79,80] also found that the obtained targets were enriched in dopaminergic synapses and serotonergic synapses. These predicted results support each other, revealing the involvement of these pathways in the treatment of SMIs, and reflecting the commonality of the pathogenesis among SMIs. Abnormal levels of DA and 5-HT are among the many causes of anxiety, depression, and other psychiatric diseases.[81,82] In the in vivo study, the levels of DA and 5-HT in the serum, hippocampus, mPFC, and amygdala of mice in the anxious state were higher than those of the control mice. These results are in agreement with several studies on different anxiety models, which confirmed elevated 5-HT and DA levels

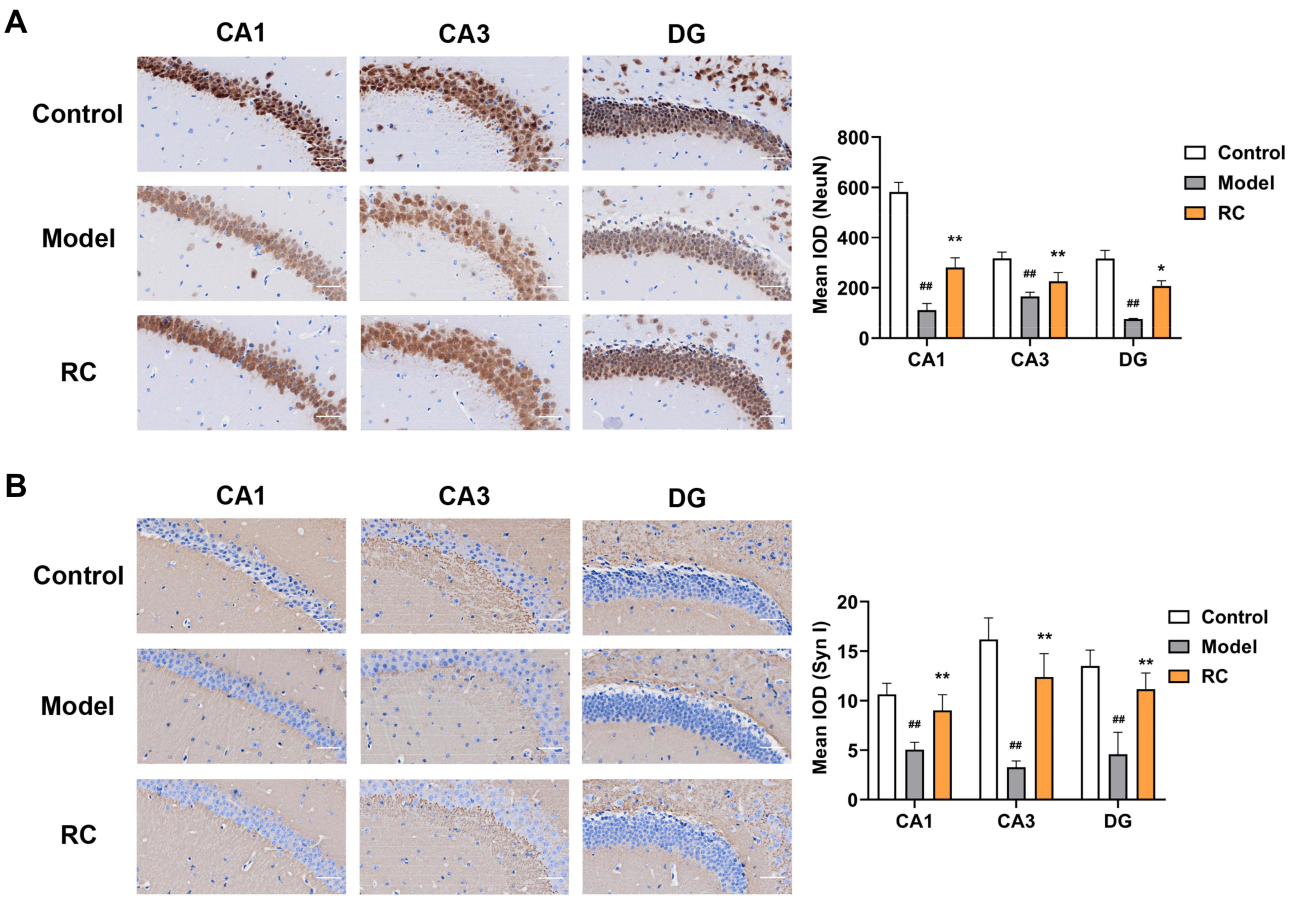

Figure 8 Effect of RC extract on NeuN and SynI levels in LPS-induced anxiety mice. Representative immunohistochemistry of (**A**) NeuN and (**B**) SynI levels in the CA1, CA3, and DG area of control, model, and RC group mice; scale bar, 50 μm. Staining was quantified by mean IOD. Data are from 6 random images per section and n=4 mice per group. Mean±SD plotted (Control vs Model, $^{\#\#}p<0.01$; Model vs RC, $^{*}p<0.05$, $^{**}p<0.01$).

in brain tissues in 1-(3-chlorophenyl) piperazine monohydrochloride,[83] EPM,[84] and uncertain empty bottle stimulation[85]-induced anxious rodents. In addition, in vivo data demonstrated that this abnormal increase in 5-HT and DA levels was restored after treatment with RC extract, validating the predicted important role of dopaminergic synapses and serotonergic synapses in *C. chinensis* Franch. therapy for SMIs here. Berberine and its derivatives have been proved to exhibit anti-anxiety effects and reduced the contents of DA and 5-HT in brain to varying degrees.[86] In fact, the C-T network diagram shows multiple components of *C. chinensis* Franch. interacting with relevant targets of dopaminergic synapses and serotonergic synapses. Hence, the neurotransmitter modulating effect of *C. chinensis* Franch. is a manifestation of multi-component synergy.

Neuronal survival and synaptic function are involved in the pathological process of SMIs. In people with psychiatric diseases, there are fewer neurons in the hippocampus.[87] In addition, damage to hippocampal neurons is a key part of the plasticity regulation of synapses.[88] At the molecular level, altered synaptic plasticity is a typical feature of the pathology of SMIs.[89,90] In an anxious depression rat model established by chronic binding stress combined with corticosterone, the average fluorescence intensity of Syn I was significantly reduced.[91] In addition, the protein expression and mRNA expression of Syn I were reduced in anxiety rats induced by nonylphenol.[92] Likewise, systematic analysis of the networks established in present studies indicated that SMI-related targets ultimately affect neuroprotection and synaptic plasticity. The predictions were confirmed by subsequent immunohistochemical experiments, which showed that the number of hippocampal neurons and the expression of synaptic plasticity protein were evidently decreased in anxious mice. These findings are consistent with the existing studies mentioned above. After treatment with RC extract, the loss of neurons and the plasticity of synapses were significantly improved.

According to the results of the current network pharmacology study, the targets of *C. chinensis* Franch. treatment for SMIs are enriched in neuroinflammation, which has been proved to be closely related to SMIs in previous studies.[93–95] Elevated levels of TNF-α and IL-1 have been reported after injection of LPS, along with an increased state of anxiety.[96] Similarly, in present animal experiments, the levels of pro-inflammatory factors (IL-1β, TNF-α) were increased, and the levels of anti-inflammatory factors (IL-4, IL-10) were decreased in brain tissue and serum in anxious mice. These events were reversed after RC extract intervention. Previously, berberine has been found to exert its anti-inflammatory effect by inhibition of the NF-κB signaling pathway.[97] Coptisine effectively inhibits the production of pro-inflammatory mediators both in vitro and in vivo by a mechanism different from berberine.[98] In addition, other alkaloid components in *C. chinensis* Franch., such as palmatine and jatrorrhizine, have also been shown to have anti-inflammatory effects.[99,100] These data further support the anti-inflammatory effects of RC extracts observed in this study, which may be achieved through the synergistic action of multiple active ingredients.

HTR2A is one of the important serotonin receptors, which affects various physiological activities by regulating the release and delivery of neurotransmitters, and is the main target associated with psychiatric disorders.[101,102] In the current study, HTR2A was predicted to be a key target for *C. chinensis* Franch. treatment of SMIs. This result is in agreement with the study of Jia et al, who predicted that HTR2A is an important protein target of Roman chamomile for the treatment of anxiety disorders, and its expression was significantly increased in the hippocampus of anxious rats.[103] The present molecular docking showed that berberine, epiberberine, palmatine, and coptisine had good affinity with HTR2A. From the date, the binding free energies of the four compounds with HTR2A were different, despite their very similar structures. Berberine and palmatine have methyl groups at R9 and R10, whereas coptisine and epiberberine have a dimethoxy group between the same site, respectively; epiberberine and palmatine have methyl groups at R2 and R3, whereas coptisine and berberine have a dimethoxy group between the same sites, respectively. Comparison of the structural characteristics of the four ingredients suggests that the number and location of methyl groups may affect the binding ability with HTR2A. The MM-PB(GB)SA calculations performed within the gmx_mmpbsa community revealed that Val156, Leu228, Phe339, and Val366 contributed significantly to the binding free energy in the four complexes. Of note, these hydrophobic amino acid residues formed pi-alkyl interactions with the benzene and pyridine ring of berberine, epiberberine, palmatine, and coptisine. The findings could be exploited further in designing future ligands from natural sources.

This study revealed the possible targets and pathways of *C. chinensis* Franch. in the treatment of SMIs, and verified its anti-anxiety efficacy and mechanism in animal experiments. However, protein-ligand binding analysis is needed to carry out to verify the molecular docking results and further determine the thermodynamic and kinetic parameters of the bindings. In addition, molecular biological studies on receptor signal transduction and gene transcription pathways were not considered, which requires further research. Taking these findings into consideration provides a basis for further development of new anti-SMIs drugs using *C. chinensis* Franch. as the base substance.

Conclusion

Combined with network pharmacology analysis, molecular docking analysis, MD simulation, and in vivo experimental validation, this study found that *C. chinensis* Franch. exerts anti-SMIs effects through its multiple active compounds acting on key target. This method adapts to the urgent need for a systematic research method of TCM, and can reveal the mystery of the synergistic effect of TCM on disease treatment. The results showed that berberine-HTR2A, epiberberine-HTR2A, palmatine-HTR2A, and coptisine-HTR2A might exert important roles. More importantly, these four compounds may be used as lead compounds for further structural modification and development. These findings will further reveal the molecular biological mechanism of *C. chinensis* Franch. treatment for SMIs. With the recognition of TCM in the world, it is a positive strategy to fill the current research gaps to organically combine TCM's understanding of the etiology and pathogenesis of emotional diseases with modern psychiatry theories.

Abbreviations

ADME, absorption, distribution, metabolism, and excretion; BP, biological process; cAMP, cyclic adenosine monophosphate; CC, cellular component; *C. chinensis* Franch., *Coptis chinensis* Franch.; CI, contribution index; C-T, compound-

target; DA, dopamine; DG, dentate gyrus; DL, drug-likeness; DZP, diazepam; EPM, elevated plus maze; GO, Gene Ontology; 5-HT, 5-hydroxytryptamine; IL, interleukin; IOD, optical density; KEGG, Kyoto Encyclopedia of Genes and Genomes; LDB, light–dark box; LPS, lipopolysaccharide; MAPK, mitogen-activated protein kinase; MD, molecular dynamics; MF, molecular function; mPFC, medial prefrontal cortex; NE, network-based; NeuN, neuron-specific nuclear protein; OB, oral bioavailability; OF, open field; RC, Rhizoma Coptidis; RIA, radioimmunoassay; RMSD, root mean square deviation; RMSF, root mean square fluctuation; SMI, serious mental illness; Syn I, synapsin I; TCM, traditional Chinese medicine; TNF-α, tumor necrosis factor-α; T-P, target-pathway.

Funding

This research was financially supported by the National Natural Science Foundation of China (Project Nos. 81873027; 81573635), the Qing-Lan Project of Jiangsu Province, the Open Project Program of Jiangsu Key Laboratory for Pharmacology and Safety Evaluation of Chinese Materia Medica (No. JKLPSE201820), the Project Funded by the Priority Academic Program Development of Jiangsu Higher Education Institutions (PAPD), the Project of the Innovation Research Team of Nanjing University of Chinese Medicine, and the Project Funded by the Six Talent Project in Jiangsu Province.

Disclosure

The authors declare that they have no competing interests.

References

1. Quirk H, Crank H, Harrop D, Hock E, Copeland R. Understanding the experience of initiating community-based physical activity and social support by people with serious mental illness: a systematic review using a meta-ethnographic approach. *Syst Rev*. 2017;6:214. doi:10.1186/s13643-017-0596-2
2. Kessler RC, Ruscio AM, Shear K, Wittchen HU. Epidemiology of anxiety disorders. *Curr Top Behav Neurosci*. 2010;2:21–35.
3. Dean J, Keshavan M. The neurobiology of depression: an integrated view. *Asian J Psychiatr*. 2017;27:101–111. doi:10.1016/j.ajp.2017.01.025
4. Kessler RC, Angermeyer M, Anthony JC, et al. Lifetime prevalence and age-of-onset distributions of mental disorders in the World Health Organization's World Mental Health Survey Initiative. *World Psychiatry*. 2007;6:168–176.
5. Perrine SA, Ghoddoussi F, Michaels MS, et al. Ketamine reverses stress-induced depression-like behavior and increased GABA levels in the anterior cingulate: an 11.7 T 1H-MRS study in rats. *Prog Neuropsychopharmacol Biol Psychiatry*. 2014;51:9–15. doi:10.1016/j.pnpbp.2013.11.003
6. Newton R, Rouleau A, Nylander AG, et al. Diverse definitions of the early course of schizophrenia-a targeted literature review. *NPJ Schizophr*. 2018;4:21. doi:10.1038/s41537-018-0063-7
7. O'Leary DS, Flaum M, Kesler ML, et al. Cognitive correlates of the negative, disorganized, and psychotic symptom dimensions of schizophrenia. *J Neuropsychiatry Clin Neurosci*. 2000;12(1):4–15. doi:10.1176/jnp.12.1.4
8. Mellman TA. Sleep and anxiety disorders. *Psychiatr Clin North Am*. 2006;29(4):1047–1058; abstract x. doi:10.1016/j.psc.2006.08.005
9. Kessler RC, Gruber M, Hettema J, et al. Co-morbid major depression and generalized anxiety disorders in the national comorbidity survey follow-up. *Psychol Med*. 2008;38(3):365–374. doi:10.1017/S0033291707002012
10. Roane BM, Taylor DJ. Adolescent insomnia as a risk factor for early adult depression and substance abuse. *Sleep*. 2008;31:1351–1356.
11. Magalhaes AC, KD Holmes, LB Dale, et al. CRF receptor 1 regulates anxiety behavior via sensitization of 5-HT2 receptor signaling. *Nat Neurosci*. 2010;13(5):622–629. doi:10.1038/nn.2529
12. Zhou Z, Zhu G, Hariri AR, et al. Genetic variation in human NPY expression affects stress response and emotion. *Nature*. 2008;452(7190):997–1001. doi:10.1038/nature06858
13. Rakofsky JJ, Dunlop BW. Treating nonspecific anxiety and anxiety disorders in patients with bipolar disorder: a review. *J Clin Psychiatry*. 2011;72(01):81–90. doi:10.4088/JCP.09r05815gre
14. Provencher MD, Hawke LD, Thienot E. Psychotherapies for comorbid anxiety in bipolar spectrum disorders. *J Affect Disord*. 2011;133(3):371–380. doi:10.1016/j.jad.2010.10.040
15. Sareen J, Jacobi F, Cox BJ, et al. Disability and poor quality of life associated with comorbid anxiety disorders and physical conditions. *Arch Intern Med*. 2006;166(19):2109–2116. doi:10.1001/archinte.166.19.2109
16. Coupland C, Dhiman P, Morriss R, et al. Antidepressant use and risk of adverse outcomes in older people: population based cohort study. *BMJ*. 2011;343:d4551. doi:10.1136/bmj.d4551
17. Wang YN, Hou Y-Y, Sun M-Z, et al. Behavioural screening of zebrafish using neuroactive traditional Chinese medicine prescriptions and biological targets. *Sci Rep*. 2014;4(1):5311. doi:10.1038/srep05311
18. Lam RW. Sleep disturbances and depression: a challenge for antidepressants. *Int Clin Psychopharmacol*. 2006;21 Suppl 1:S25–29. doi:10.1097/01.yic.0000195658.91524.61
19. Serretti A, Chiesa A. Treatment-emergent sexual dysfunction related to antidepressants: a meta-analysis. *J Clin Psychopharmacol*. 2009;29(3):259–266. doi:10.1097/JCP.0b013e3181a5233f
20. Serretti A, Mandelli L. Antidepressants and body weight: a comprehensive review and meta-analysis. *J Clin Psychiatry*. 2010;71(10):1259–1272. doi:10.4088/JCP.09r05346blu

21. Anderson HD, Pace WD, Libby AM, West DR, Valuck RJ. Rates of 5 common antidepressant side effects among new adult and adolescent cases of depression: a retrospective US claims study. *Clin Ther*. 2012;34(1):113–123. doi:10.1016/j.clinthera.2011.11.024
22. Jiang WY. Therapeutic wisdom in traditional Chinese medicine: a perspective from modern science. *Trends Pharmacol Sci*. 2005;26 (11):558–563. doi:10.1016/j.tips.2005.09.006
23. Lee B, Sur B, Yeom M, et al. Effect of berberine on depression- and anxiety-like behaviors and activation of the noradrenergic system induced by development of morphine dependence in rats. *Korean J Physiol Pharmacol*. 2012;16(6):379–386. doi:10.4196/kjpp.2012.16.6.379
24. Hu Y, Ehli EA, Hudziak JJ, Davies GE. Berberine and evodiamine influence serotonin transporter (5-HTT) expression via the 5-HTT-linked polymorphic region. *Pharmacogenomics J*. 2012;12(5):372–378. doi:10.1038/tpj.2011.24
25. Kulkarni SK, Dhir A. Berberine: a plant alkaloid with therapeutic potential for central nervous system disorders. *Phytother Res*. 2010;24:317–324. doi:10.1002/ptr.2968
26. Xu F, Yang J, Meng B, et al. [The effect of berberine on ameliorating chronic inflammatory pain and depression]. *Zhonghua Yi Xue Za Zhi*. 2018;98:1103–1108. Chinese. doi:10.3760/cma.j.issn.0376-2491.2018.14.011
27. Zhe Q, Sulei W, Weiwei T, Hongyan L, Jianwei W. Effects of Jiaotaiwan on depressive-like behavior in mice after lipopolysaccharide administration. *Metab Brain Dis*. 2017;32(2):415–426. doi:10.1007/s11011-016-9925-8
28. Zhu X, Sun Y, Zhang C, Liu H. Effects of berberine on a rat model of chronic stress and depression via gastrointestinal tract pathology and gastrointestinal flora profile assays. *Mol Med Rep*. 2017;15(5):3161–3171. doi:10.3892/mmr.2017.6353
29. Ru J, Li P, Wang J, et al. TCMSP: a database of systems pharmacology for drug discovery from herbal medicines. *J Cheminform*. 2014;6(1):13. doi:10.1186/1758-2946-6-13
30. Yao Y, Zhang X, Wang Z, et al. Deciphering the combination principles of Traditional Chinese Medicine from a systems pharmacology perspective based on Ma-huang decoction. *J Ethnopharmacol*. 2013;150(2):619–638. doi:10.1016/j.jep.2013.09.018
31. Yue SJ, Liu J, Feng -W-W, et al. System pharmacology-based dissection of the synergistic mechanism of Huangqi and Huanglian for diabetes mellitus. *Front Pharmacol*. 2017;8:694. doi:10.3389/fphar.2017.00694
32. Liu Z, Guo F, Wang Y, et al. BATMAN-TCM: a bioinformatics analysis tool for molecular mechANism of Traditional Chinese Medicine. *Sci Rep*. 2016;6:21146. doi:10.1038/srep21146
33. Wang X, Shen Y, Wang S, et al. PharmMapper 2017 update: a web server for potential drug target identification with a comprehensive target pharmacophore database. *Nucleic Acids Res*. 2017;45(W1):W356–W360. doi:10.1093/nar/gkx374
34. Gfeller D, Grosdidier A, Wirth M, et al. SwissTargetPrediction: a web server for target prediction of bioactive small molecules. *Nucleic Acids Res*. 2014;42(W1):W32–38. doi:10.1093/nar/gku293
35. Szklarczyk D, Santos A, von Mering C, et al. STITCH 5: augmenting protein-chemical interaction networks with tissue and affinity data. *Nucleic Acids Res*. 2016;44(D1):D380–384. doi:10.1093/nar/gkv1277
36. Zhu F, Shi Z, Qin C, et al. Therapeutic target database update 2012: a resource for facilitating target-oriented drug discovery. *Nucleic Acids Res*. 2012;40(D1):D1128–1136. doi:10.1093/nar/gkr797
37. Pinero J, Bravo À, Queralt-Rosinach N, et al. DisGeNET: a comprehensive platform integrating information on human disease-associated genes and variants. *Nucleic Acids Res*. 2017;45(D1):D833–D839. doi:10.1093/nar/gkw943
38. Amberger JS, Bocchini CA, Schiettecatte F, Scott AF, Hamosh A. OMIM.org: online Mendelian Inheritance in Man (OMIM(R)), an online catalog of human genes and genetic disorders. *Nucleic Acids Res*. 2015;43(D1):D789–798. doi:10.1093/nar/gku1205
39. Huang DW, Sherman BT, Tan Q, et al. DAVID bioinformatics resources: expanded annotation database and novel algorithms to better extract biology from large gene lists. *Nucleic Acids Res*. 2007;35:W169–175. doi:10.1093/nar/gkm415
40. Smoot ME, Ono K, Ruscheinski J, Wang PL, Ideker T. Cytoscape 2.8: new features for data integration and network visualization. *Bioinformatics*. 2011;27(3):431–432. doi:10.1093/bioinformatics/btq675
41. Yue SJ, Xin L-T, Fan Y-C, et al. Herb pair Danggui-Honghua: mechanisms underlying blood stasis syndrome by system pharmacology approach. *Sci Rep*. 2017;7(1):40318. doi:10.1038/srep40318
42. Trott O, Olson AJ. AutoDock Vina: improving the speed and accuracy of docking with a new scoring function, efficient optimization, and multithreading. *J Comput Chem*. 2010;31:455–461. doi:10.1002/jcc.21334
43. Pettersen EF, Goddard TD, Huang CC, et al. UCSF Chimera–a visualization system for exploratory research and analysis. *J Comput Chem*. 2004;25(13):1605–1612. doi:10.1002/jcc.20084
44. Wang J, Wolf RM, Caldwell JW, Kollman PA, Case DA. Development and testing of a general amber force field. *J Comput Chem*. 2004;25 (9):1157–1174. doi:10.1002/jcc.20035
45. Lu T, Chen F. Multiwfn: a multifunctional wavefunction analyzer. *J Comput Chem*. 2012;33(5):580–592. doi:10.1002/jcc.22885
46. Jorgensen WL, Chandrasekhar J, Madura JD, Impey RW, Klein ML. Comparison of simple potential functions for simulating liquid water. *J Comput Phys*. 1983;79:926–935. doi:10.1063/1.445869
47. Maier JA, Martinez C, Kasavajhala K, et al. ff14SB: improving the accuracy of protein side chain and backbone parameters from ff99SB. *J Chem Theory Comput*. 2015;11(8):3696–3713. doi:10.1021/acs.jctc.5b00255
48. Larini L, Mannella R, Leporini D. Langevin stabilization of molecular-dynamics simulations of polymers by means of quasisymplectic algorithms. *J Chem Phys*. 2007;126(10):104101. doi:10.1063/1.2464095
49. Berendsen HJC, Postma JPM, van Gunsteren WF, DiNola A, Haak JR. Molecular dynamics with coupling to an external bath. *J Chem Phys*. 1984;81(8):3684–3690. doi:10.1063/1.448118
50. Van Der Spoel D, Lindahl E, Hess B, et al. GROMACS: fast, flexible, and free. *J Comput Chem*. 2005;26:1701–1718. doi:10.1002/jcc.20291
51. Valdes-Tresanco MS, Valdes-Tresanco ME, Valiente PA, Moreno E. gmx_MMPBSA: a new tool to perform end-state free energy calculations with GROMACS. *J Chem Theory Comput*. 2021;17(10):6281–6291. doi:10.1021/acs.jctc.1c00645
52. Guo S, Shen QN, Cao HH, et al. [Study on quality of standard decoction of Coptidis Rhizoma based on traditional decoction process]. *Zhongguo Zhong Yao Za Zhi*. 2019;44:3985–3993. Chinese. doi:10.19540/j.cnki.cjcmm.20190630.303
53. Savignac HM, Couch Y, Stratford M, et al. Prebiotic administration normalizes lipopolysaccharide (LPS)-induced anxiety and cortical 5-HT2A receptor and IL1-beta levels in male mice. *Brain Behav Immun*. 2016;52:120–131. doi:10.1016/j.bbi.2015.10.007
54. Committee SP. *Chinese Pharmacopoeia 2020*. China Medical Science Press; 2020.

55. Dantzer R, O'Connor JC, Freund GG, Johnson RW, Kelley KW. From inflammation to sickness and depression: when the immune system subjugates the brain. *Nat Rev Neurosci*. 2008;9(1):46–57. doi:10.1038/nrn2297
56. Prut L, Belzung C. The open field as a paradigm to measure the effects of drugs on anxiety-like behaviors: a review. *Eur J Pharmacol*. 2003;463 (1–3):3–33. doi:10.1016/s0014-2999(03)01272-x
57. Jangra A, Lukhi MM, Sulakhiya K, Baruah CC, Lahkar M. Protective effect of mangiferin against lipopolysaccharide-induced depressive and anxiety-like behaviour in mice. *Eur J Pharmacol*. 2014;740:337–345. doi:10.1016/j.ejphar.2014.07.031
58. Savalli G, Diao W, Berger S, et al. Anhedonic behavior in cryptochrome 2-deficient mice is paralleled by altered diurnal patterns of amygdala gene expression. *Amino Acids*. 2015;47(7):1367–1377. doi:10.1007/s00726-015-1968-3
59. Leach G, Adidharma W, Yan L, Yamazaki S. Depression-like responses induced by daytime light deficiency in the diurnal grass rat (Arvicanthis niloticus). *PLoS One*. 2013;8(2):e57115. doi:10.1371/journal.pone.0057115
60. Cicvaric A, Sachernegg HM, Stojanovic T, et al. Podoplanin gene disruption in mice promotes in vivo neural progenitor cells proliferation, selectively impairs dentate gyrus synaptic depression and induces anxiety-like behaviors. *Front Cell Neurosci*. 2019;13:561. doi:10.3389/fncel.2019.00561
61. Cicvaric A, Bulat T, Bormann D, et al. Sustained consumption of cocoa-based dark chocolate enhances seizure-like events in the mouse hippocampus. *Food Funct*. 2018;9(3):1532–1544. doi:10.1039/c7fo01668a
62. Walf AA, Frye CA. The use of the elevated plus maze as an assay of anxiety-related behavior in rodents. *Nat Protoc*. 2007;2(2):322–328. doi:10.1038/nprot.2007.44
63. Hayashi Y, Sogabe S, Hattori Y, Tanaka J. Anxiolytic and hypnotic effects in mice of roasted coffee bean volatile compounds. *Neurosci Lett*. 2012;531:166–169. doi:10.1016/j.neulet.2012.10.044
64. Sutthibutpong T, Rattanarojpong T, Khunrae P. Effects of helix and fingertip mutations on the thermostability of xyn11A investigated by molecular dynamics simulations and enzyme activity assays. *J Biomol Struct Dyn*. 2018;36(15):3978–3992. doi:10.1080/07391102.2017.1404934
65. Liu J, Wei B, Che C,et al. Enhanced stability of manganese superoxide dismutase by amino acid replacement designed via molecular dynamics simulation. *Int J Biol Macromol*. 2019;128:297–303. doi:10.1016/j.ijbiomac.2019.01.126
66. Arab Z, Hosseini M, Mashayekhi F, Anaeigoudari A. Zataria multiflora extract reverses lipopolysaccharide-induced anxiety and depression behaviors in rats. *Avicenna J Phytomed*. 2020;10:78–88.
67. Alzarea S, Rahman S. Alpha-7 nicotinic receptor allosteric modulator PNU120596 prevents lipopolysaccharide-induced anxiety, cognitive deficit and depression-like behaviors in mice. *Behav Brain Res*. 2019;366:19–28. doi:10.1016/j.bbr.2019.03.019
68. Zhang L, Previn R, Lu L, et al. Crocin, a natural product attenuates lipopolysaccharide-induced anxiety and depressive-like behaviors through suppressing NF-kB and NLRP3 signaling pathway. *Brain Res Bull*. 2018;142:352–359. doi:10.1016/j.brainresbull.2018.08.021
69. Lee B, Shim I, Lee H, Hahm DH. Gypenosides attenuate lipopolysaccharide-induced neuroinflammation and anxiety-like behaviors in rats. *Anim Cells Syst*. 2018;22(5):305–316. doi:10.1080/19768354.2018.1517825
70. Li M, Li C, Yu H, et al. Lentivirus-mediated interleukin-1beta (IL-1beta) knock-down in the hippocampus alleviates lipopolysaccharide (LPS)-induced memory deficits and anxiety- and depression-like behaviors in mice. *J Neuroinflammation*. 2017;14:190. doi:10.1186/s12974-017-0964-9
71. Yu M, Yang D, Wang M, Wei X, Li W. Early stage of diffusional kurtosis imaging and dynamic contrast-enhanced magnetic resonance imaging correlated with long-term neurocognitive function after experimental traumatic brain injury. *Neurosci Lett*. 2019;705:206–211. doi:10.1016/j.neulet.2019.04.034
72. Lin YS, Wang H-Y, Huang D-F, et al. Neuronal splicing regulator RBFOX3 (NeuN) regulates adult hippocampal neurogenesis and synaptogenesis. *PLoS One*. 2016;11(10):e0164164. doi:10.1371/journal.pone.0164164
73. Qi YY, Zhang QC, Zhu HX. Huang-Lian Jie-Du decoction: a review on phytochemical, pharmacological and pharmacokinetic investigations. *Chin Med*. 2019;14:57. doi:10.1186/s13020-019-0277-2
74. Liu Q, Wang R, Zhao MF, Fan SL. Clinical observation of Jiajian Huanglian Wendan decoction for liver stagnation and phlegm type generalized anxiety. *Chin Pharm*. 2016;27:1984–1986.
75. Chang JH, Sun GC. Clinical observation on treating 60 cases of anxiety disorder patients with the Huanglian Ejiao decoction plus fluvoxamine. *Clin J Chin Med*. 2012;4:97–98. doi:10.3969/j.issn.1674-7860.2012.16.057
76. Zhang ZY, Lin JY, Zhou D. Clinical effect of Huanglian Ejiao Decoction on insomnia with Yin deficiency and fire flourishing syndrome and its effect on levels of serotonin and dopamine. *Chin Arch Trad Chin Med*. 2021;39:167–171.
77. Lee B, Shim I, Lee H, Hahm DH. Berberine alleviates symptoms of anxiety by enhancing dopamine expression in rats with post-traumatic stress disorder. *Korean J Physiol Pharmacol*. 2018;22(2):183–192. doi:10.4196/kjpp.2018.22.2.183
78. Ghotbi Ravandi S, Shabani M, Bashiri H, et al. Ameliorating effects of berberine on MK-801-induced cognitive and motor impairments in a neonatal rat model of schizophrenia. *Neurosci Lett*. 2019;706:151–157. doi:10.1016/j.neulet.2019.05.029
79. Bai YT, Zhang Y, Li S, et al. Integrated network pharmacology analysis and experimental validation to investigate the mechanism of Zhi-Zi-Hou-Po decoction in depression. *Front Pharmacol*. 2021;12. doi:10.3389/fphar.2021.711303
80. Liu PL, Song A-R, Dong C-D, et al. Network pharmacology study on the mechanism of the herb pair of prepared Rehmannia root-Chinese arborvitae kernel for anxiety disorders. *Ann Palliat Med*. 2021;10(3):3313–3327. doi:10.21037/apm-21-531
81. Stein DJ, Westenberg HG, Liebowitz MR. Social anxiety disorder and generalized anxiety disorder: serotonergic and dopaminergic neurocircuitry. *J Clin Psychiatry*. 2002;63 Suppl 6:12–19.
82. Lowry CA, Johnson PL, Hay-Schmidt A, Mikkelsen J, Shekhar A. Modulation of anxiety circuits by serotonergic systems. *Stress*. 2005;8 (4):233–246. doi:10.1080/10253890500492787
83. Zhang WJ, Han QY, Xu CJ. Effect of 20(S)-protopanaxadiol on the ethology in the anxiety model mice and neurotransmitter and certain gene expression in its brain. *Chin J Clin Pharm*. 2015;24:220–227. doi:10.19577/j.cnki.issn10074406.2015.04.003
84. Li JJ, Tang JL, Hu LL, Zhou SW, Zhou JY. Effect of rhynchophylla total alkaloids on behavior and contents of monoamine neurotransmitters in brain tissues of anxiety model rats. *J Third Mil Med Univ*. 2013;35:237–240. doi:10.16016/j.1000-5404.2013.03.007
85. Feng GK, Ma XJ, Chen YY, et al. Effects of Chailong Jieyu Pill on monoamine neurotransmitters in rat models with anxiety disorder. *J Liaoning Univ TCM*. 2017;19:16–18. doi:10.13194/j.issn.1673-842x.2017.11.004
86. Pang J, et al. Influence of 8-alkyl-berberine on ethology and neurotransmitter in brain tissue of anxiety model mice. *Chin Tradit Herb Drugs*. 2014;45:2953–2957.

87. Pelkey KA, Chittajallu R, Craig MT, et al. Hippocampal GABAergic inhibitory interneurons. *Physiol Rev*. 2017;97:1619–1747. doi:10.1152/physrev.00007.2017
88. Zhou B, Tan J, Zhang C, Wu Y. Neuroprotective effect of polysaccharides from Gastrodia elata blume against corticosterone-induced apoptosis in PC12 cells via inhibition of the endoplasmic reticulum stress-mediated pathway. *Mol Med Rep*. 2018;17:1182–1190. doi:10.3892/mmr.2017.7948
89. Carter CJ. eIF2B and oligodendrocyte survival: where nature and nurture meet in bipolar disorder and schizophrenia? *Schizophr Bull*. 2007;33(6):1343–1353. doi:10.1093/schbul/sbm007
90. Schmitt A, Hasan A, Gruber O, Falkai P. Schizophrenia as a disorder of disconnectivity. *Eur Arch Psychiatry Clin Neurosci*. 2011;261 Suppl 2(S2):S150–154. doi:10.1007/s00406-011-0242-2
91. Zhao HQ, Liu J, Meng P, et al. [Effect of Baihe Dihuang Decoction on synaptic plasticity of hippocampus in rats with anxious depression]. *Zhongguo Zhong Yao Za Zhi*. 2021;46:1205–1210. Chinese. doi:10.19540/j.cnki.cjcmm.20201221.401
92. Li S, Xu W, Gong L, et al. Subchronic nonylphenol exposure induced anxiety-like behavior and decreased expressions of regulators of synaptic plasticity in rats. *Chemosphere*. 2021;282:130994. doi:10.1016/j.chemosphere.2021.130994
93. Badshah H, Ali T, Kim MO. Osmotin attenuates LPS-induced neuroinflammation and memory impairments via the TLR4/NFkappaB signaling pathway. *Sci Rep*. 2016;6(1):24493. doi:10.1038/srep24493
94. Farooq RK, Asghar K, Kanwal S, Zulqernain A. Role of inflammatory cytokines in depression: focus on interleukin-1beta. *Biomed Rep*. 2017;6(1):15–20. doi:10.3892/br.2016.807
95. Yue N, Huang H, Zhu X, et al. Activation of P2X7 receptor and NLRP3 inflammasome assembly in hippocampal glial cells mediates chronic stress-induced depressive-like behaviors. *J Neuroinflammation*. 2017;14:102. doi:10.1186/s12974-017-0865-y
96. Kullmann JS, Grigoleit J-S, Lichte P, et al. Neural response to emotional stimuli during experimental human endotoxemia. *Hum Brain Mapp*. 2013;34(9):2217–2227. doi:10.1002/hbm.22063
97. Jiang Q, Liu P, Wu X, et al. Berberine attenuates lipopolysaccharide-induced extracellular matrix accumulation and inflammation in rat mesangial cells: involvement of NF-kappaB signaling pathway. *Mol Cell Endocrinol*. 2011;331(1):34–40. doi:10.1016/j.mce.2010.07.023
98. Wu J, Zhang H, Hu B, et al. Coptisine from Coptis chinensis inhibits production of inflammatory mediators in lipopolysaccharide-stimulated RAW 264.7 murine macrophage cells. *Eur J Pharmacol*. 2016;780:106–114. doi:10.1016/j.ejphar.2016.03.037
99. Li JY, Wang XB, Luo JG, Kong LY. Seasonal variation of alkaloid contents and anti-inflammatory activity of Rhizoma coptidis based on fingerprints combined with chemometrics methods. *J Chromatogr Sci*. 2015;53:1131–1139. doi:10.1093/chromsci/bmu175
100. Lee WC, Kim J-K, Kang J-W, et al. Palmatine attenuates D-galactosamine/lipopolysaccharide-induced fulminant hepatic failure in mice. *Food Chem Toxicol*. 2010;48(1):222–228. doi:10.1016/j.fct.2009.10.004
101. Mestre TA, Zurowski M, Fox SH. 5-Hydroxytryptamine 2A receptor antagonists as potential treatment for psychiatric disorders. *Expert Opin Inv Drug*. 2013;22(4):411–421. doi:10.1517/13543784.2013.769957
102. Aznar S, Hervig ME. The 5-HT2A serotonin receptor in executive function: implications for neuropsychiatric and neurodegenerative diseases. *Neurosci Biobehav REV*. 2016;64:63–82. doi:10.1016/j.neubiorev.2016.02.008
103. Jia Y, Zou J, Wang Y, et al. Action mechanism of Roman chamomile in the treatment of anxiety disorder based on network pharmacology. *J Food Biochem*. 2021;45(1):e13547. doi:10.1111/jfbc.13547